environmental microbiology

Environmental Microbiology (2012) doi:10.1111/j.1462-2920.2012.02745.x

# *In situ* survey of life cycle phases of the coccolithophore *Emiliania huxleyi* (*Haptophyta*)

**Miguel J. Frada,[1,2]* Kay D. Bidle,[3] Ian Probert[1] and Colomban de Vargas[1]**

[1]*CNRS and Université de Pierre et Marie Curie (Paris 06), UMR 7144, EPPO team, Station Biologique de Roscoff, 29682 Roscoff, France.*

[2]*Centro de Geologia, Departamento de Geologia, Faculdade de Ciências, Universidade de Lisboa, Edifício C6, Campo Grande, 1749-016 Lisboa, Portugal.*

[3]*Environmental Biophysics and Molecular Ecology Group, Institute of Marine and Coastal Sciences, Rutgers University, 71 Dudley Road, New Brunswick, NJ 08901, USA.*

## Summary

**The cosmopolitan coccolithophore *Emiliania huxleyi* is characterized by a strongly differentiated haplodiplontic life cycle consisting of a diploid phase, generally bearing coccoliths (calcified) but that can be also non-calcified, and a non-calcified biflagellated haploid phase. Given most studies have focused on the bloom-producing calcified phase, there is little-to-no information about non-calcified cells in nature. Using field mesocoms as experimental platforms, we quantitatively surveyed calcified and non-calcified cells using the combined calcareous detection fluorescent *in situ* hybridization (COD-FISH) method and qualitatively screened for haploid specific transcripts using reverse transcription-PCR during *E. huxleyi* bloom successions. Diploid, calcified cells formed dense blooms that were followed by the massive proliferation of *E. huxleyi* viruses (*Eh*Vs), which caused bloom demise. Non-calcified cells were also detected throughout the experiment, accounting for a minor fraction of the population but becoming progressively more abundant during mid-late bloom periods concomitant with *Eh*V burst. Non-calcified cell growth also paralleled a distinct window of haploid-specific transcripts and the appearance of autotrophic flagellates morphologically similar to haploid cells, both of which are suggestive of meiosis and sexual life cycling during natural blooms of this prominent marine phytoplankton species.**

Received 12 November, 2011; revised 10 March, 2012; accepted 12 March, 2012. *For correspondence. E-mail miguel.frada@weizmann.ac.il; Tel. (+972) 89342914; Fax (+972) 89344181.

## Introduction

*Emiliania huxleyi* (Lohmann) Hay and Mohler (*Prymnesiophyceae*, *Haptophyta*) is a highly diverse and ubiquitously distributed coccolithophore morphospecies (Winter *et al.*, 1994; Iglesias-Rodriguez *et al.*, 2006; Hagino *et al.*, 2011), often constituting an important component of the marine phytoplankton assemblages (McIntyre and Bé, 1967; Okada and McIntyre, 1977; Campbell *et al.*, 1994) and forming seasonal blooms that cover vast oceanic and neritic areas worldwide (Holligan *et al.*, 1983; Brown and Yoder, 1994; Tyrrell and Merico, 2004). This massive development of *E. huxleyi* populations enhances the fluxes of important elements (oxygen, carbon, sulfur) between the atmosphere, the oceans and oceans floor, exerting a major impact on earth climate (Charlson *et al.*, 1987; Westbroek *et al.*, 1993; Malin and Steinke, 2004; Rost and Riebesell, 2004). Consequently, the ecophysiology and molecular ecology of *E. huxleyi* has been intensively studied (Paasche, 2001; von Dassow *et al.*, 2009; Rokitta *et al.*, 2011), and a whole genome sequencing project is nearing completion (http://genome.jgi-psf.org/).

A basic feature of *E. huxleyi*, shared among prymnesiophytes (Billard, 1994), is its characteristic haplodiplontic and heteromorphic life cycle composed of a diploid (2N) coccolith-bearing non-motile phase (calcified cell), a 2N non-calcified non-motile phase (naked cell), which is sometimes interpreted as a artefact of extensive cultivation periods, and a haploid (1N) non-calcified biflagellated phase bearing organic scales bound to the plasmalemma (scaly cell) and likely serving at some point as sexual gametes (Klaveness, 1972; Green *et al.*, 1996). All life cycle forms are capable of independent mitotic division producing dense cultures, but there is no insight into the timing and key factors triggering life cycle interchange, such as syngamy and meiosis. Original descriptions (along with our own observations) noticed that 1N and 2N-naked cells may form spontaneously when calcified cells become senescent, but reversion back to the calcified form was never observed (Klaveness, 1972).

Beyond a clear morphological distinction, it has recently been shown that 1N and 2N cells possess distinct physiological and genetic properties. For example, 1N cells

appear to be high light sensitive (Houdan *et al*., 2005). On the other hand, 1N cells are not susceptible to *E. huxleyi* specific viruses (*Eh*Vs) that routinely infect and kill 2N cells (Frada *et al*., 2008). Morphologically distinct 1N cells may thus be produced through meiosis and act as a resistant stage allowing species survival under viral pressure; a process metaphorically coined as the 'Cheshire cat escape strategy' (Frada *et al*., 2008). Recent transcriptome analyses have also revealed a dramatic differentiation between 1N and 2N cells with less than 50% of transcripts estimated to be common between the two phases, thereby exposing a wide array of distinct physiological abilities (von Dassow *et al*., 2009; Rokitta *et al*., 2011).

Taken together, this marked physiological differentiation strongly suggests that 2N and 1N cells may exploit different niches, displaying distinct roles in nature. Nonetheless, such claims still require verification. To date, nearly all field studies have focused solely on the 2N coccolith bearing phase largely due to the formation of extensive blooms. In contrast, field evidence of non-calcified cells (including 1N and non-calcified 2N cells) is minimal and at best fragmentary and unclear. For instance, the original descriptions by Lohmann (1902) reported non-calcified flagellated cells in natural samples, stating that they could be related to calcifying *E. huxleyi* cells based on their shape and size. More recently, Rhodes and colleagues (1995) while examining phytoplankton assemblages from the coast of New Zealand isolated calcified cells that in culture produced motile non-calcified cells. However, a clear identification of these cells was not provided in the study and no particular trigger for phase transition was identified. Campbell and co-authors (Campbell *et al*., 1994) did obtain the first total *E. huxleyi* counts during cruise transects on the north Atlantic and Pacific oceans using antibodies developed to target both calcified and non-calcified *E. huxleyi* cells (Shapiro *et al*., 1989). Unfortunately, individual calcified and non-calcified cells counts were not provided in this study. In these terms, the relative proportion and the ecological interplay over time and space between calcified and non-calcified forms as well as prevalence and role of haploid cells and frequency of sexual life cycle interchange remain unknown.

In this study, we monitored calcified and non-calcified *E. huxleyi* cells during the development of *E. huxleyi* blooms induced in offshore mesocosms (Bergen, Norway) using the COD-FISH method (Frada *et al*., 2006). We further assessed the presence of 1N-specific transcripts using recently described life cycle specific markers for *E. huxleyi* (von Dassow *et al*., 2009) as a further diagnostic of haploidy during bloom succession. Our study provides the first quantitative field-survey of non-calcified *E. huxleyi* cells in nature using a novel oligonucleotide fluorescent probe. It also unveils haploid cells in nature and furthermore provides evidence for life cycle transition via meiosis during peak bloom abundance of *E. huxleyi* diploid cells and the onset of viral demise.

## Results

### *Bloom dynamics: assessment of calcified and non-calcified* E. huxleyi *cells*

Calcified and non-calcified *E. huxleyi* cells were assessed via the COD-FISH method using a novel fluorescence probe (EG28-03) specific to *E. huxleyi* and to the sister species *Gephyrocapsa oceanica*, and not labelling other microalgae strains (Fig. S1). COD-FISH couples fluorescence *in situ* hybridization with cross-polarization microscopy, allowing for the simultaneous fluorescent labelling of calcified and non-calcified *E. huxleyi* cells within natural assemblages and optical discrimination of calcified cells (see *Experimental procedures*).

COD-FISH assessment of the surrounding fjord water prior to the mesocosm revealed ~ $2.4 \times 10^2$ to ~ $3.0 \times 10^2$ *E. huxleyi* 2N calcified cells ml$^{-1}$ and 12–26 non-calcified cells ml$^{-1}$ in the upper 10 metres (Fig. 1). This water served as the inoculum for mesocosm enclosure experiments, which were supplemented daily with $NaNO_3$ and $K_2HPO_4$ at either 15N: 1P ratio (nutrient replete, M3) or 75N: 1P ratio (phosphate limited, M2). Surveys of cells in both enclosures over 16 days revealed three major growth phases (Fig. 2): Phase 1 (days 0–7), characterized by a lagging phase with calcified cells varying from ~ $3.0 \times 10^2$ cells ml$^{-1}$ to ~ $1.4 \times 10^4$ cells ml$^{-1}$; Phase 2 (days 7–13), characterized by the marked growth of calcified cells from ~ $1.4 \times 10^4$ cells ml$^{-1}$ to a maximum of

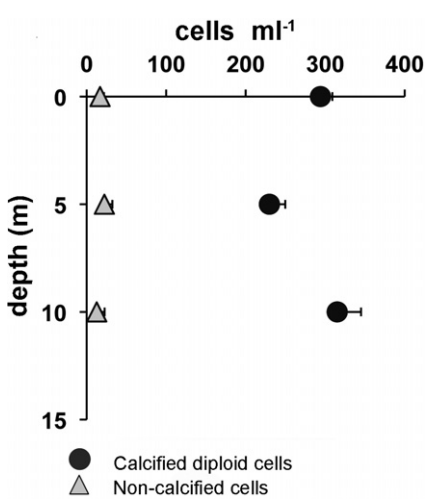


**Fig. 1.** Vertical distribution of calcified and non-calcified *E. huxleyi* cells in the upper 10 m of Raunefjorden water column. Cells were assessed with the COD-FISH method.

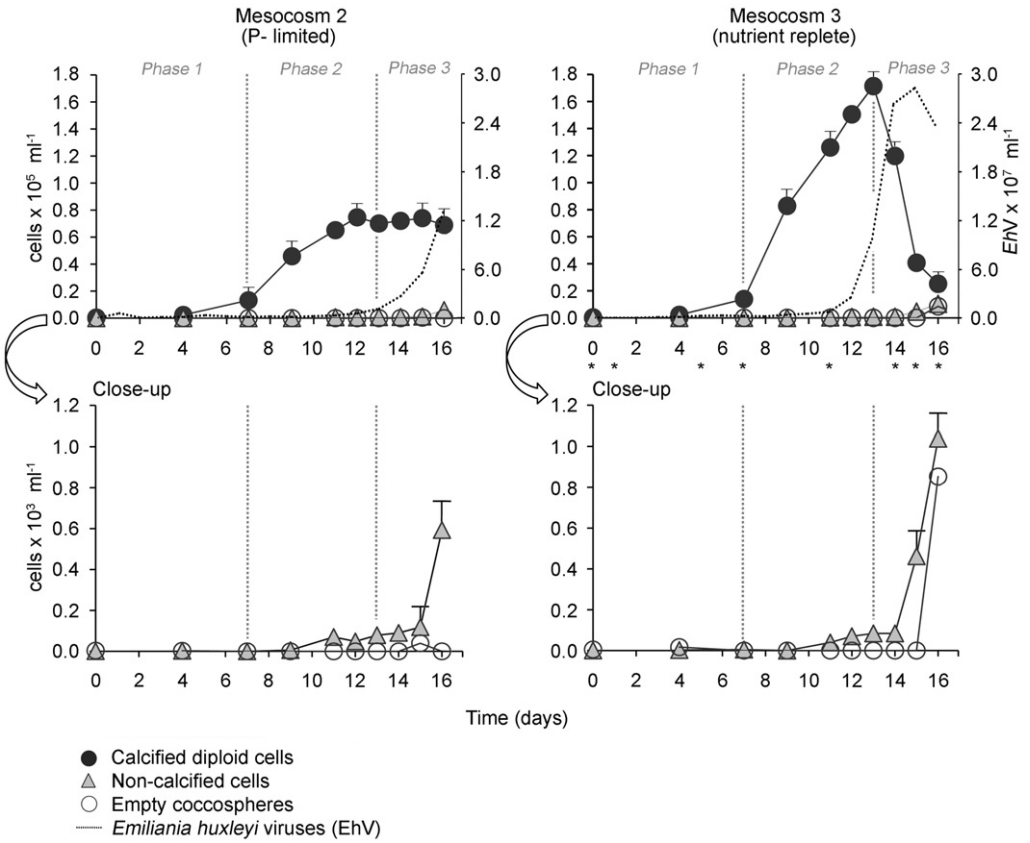


**Fig. 2.** Mesocosm blooms dynamics. Calcified and non-calcified *E. huxleyi* cells, as well as empty *E. huxleyi* coccospheres were assessed with the COD-FISH method. *Eh*V abundance was assessed by flow-cytometry (Pagarete *et al*., 2011). Bottom panels highlight the dynamics of less dense non-calcified cells and empty coccospheres, as indicated by arrows. Asterisks below M3 plot (upper right panel) indicate the time points used for reverse transcription–polymerase chain reaction (RT-PCR) (see Fig. 4 and related results).

~ $0.8 \times 10^5$ cells ml$^{-1}$ in M2 (day 12), and from ~ $1.5 \times 10^4$ cells ml$^{-1}$ to ~ $1.7 \times 10^5$ cells ml$^{-1}$ in M3 (day 13), and the initial proliferation of *Eh*Vs (virus data was retrieved from Pagarete *et al*., 2011); Phase 3 (days 13–17), characterized by stationary phase of the calcified population around $0.8 \times 10^5$ cells ml$^{-1}$ in M2, whereas in M3 calcified cells declined from ~ $1.7 \times 10^5$ cells ml$^{-1}$ in day 13 to $0.3 \times 10^5$ cells ml$^{-1}$ in day 17. At this point *Eh*Vs reached their maximal abundance of ~ $1.3 \times 10^7$ *Eh*Vs ml$^{-1}$ in M2 (day 16) and ~ $2.8 \times 10^7$ *Eh*Vs ml$^{-1}$ in M3 (day 15).

In parallel, we also detected non-calcified *E. huxleyi* cells in all mesocosm phases (Fig. 2, bottom insets). In Phase 1, these cells ranged from 25 to 50 cells ml$^{-1}$ in M2 and M3, appearing fully labelled with the EG28-03 probe (Fig. 3A). At the end of exponential growth of calcified cells, we detected the progressive development of the non-calcified pool, increasing up to ~ $1 \times 10^3$ cells ml$^{-1}$ in day 14 and 15 in M3 and M2 respectively (Fig. 2; see cells in Fig. 3D and E). Microscopic examination of fresh samples collected between days 12 and 14 also detected clusters of 2 or 3 small ($\leq 5$ μm) photosynthetic flagellated cells bound to coccolith aggregates (Fig. 3F–H, Video S1). Subsequent COD-FISH analysis from days 16 and 17 revealed the rapid accumulation of non-calcified cells together with the sudden appearance of empty *E. huxleyi* coccospheres, which did not possess chlorophyll autofluorescence and were not labelled with the fluorescent FISH probe.

### *Assessment of* E. huxleyi *specific transcripts*

The detection of non-calcified cells by COD-FISH and the observations of a few flagellates associated with coccoliths prompted us to more decisively determine the nature of these cells. We used a reverse transcription–polymerase chain reaction (RT-PCR) approach that employed *E. huxleyi* haploid specific primers (Table S1) to screen cDNA generated from mesocosm samples (M3, days 0, 1, 5, 7, 11, 14, 15, 16) for the presence 1N gene signatures. The primer sets used were specific for an elongation factor 1α targeting both 1N and 2N cells and six 1N specific primers (histone H2A, Myb family transcription factor, false agglutinin homologue, phototropin homologue, putative DNA-6-adenine methyltransferase

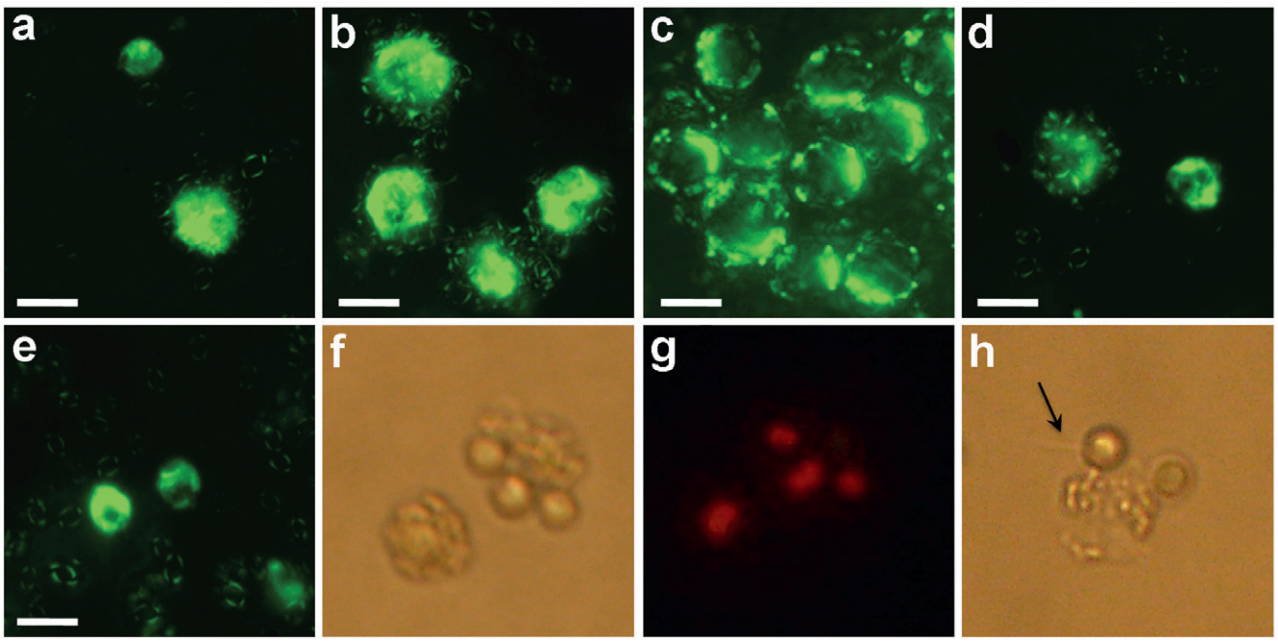


**Fig. 3.** Microscopic images of different *E. huxleyi* cell forms detected during the mesocosms.
A–E. Merged epifluorescence microscopy (490/515 nm, excitation/emission) and cross-polarized microscopy images from samples processed by COD-FISH using the *E. huxleyi* specific oligonucleotide probe EG28-03 (scale = 5 μm). (A) Non-calcified (upper cell) and calcified (lower cell) *E. huxleyi* cells on day 2. An assemblage of coccoliths covering the cell can be seen around the calcified cell. (B and C) Groups of calcified *E. huxleyi* cells on days 4 and 9 respectively). (D) Calcified (left cell) and non-calcified (right cell) *E. huxleyi* cells on day 13. (E) Two non-calcified *E. huxleyi* cells. Dispersed coccoliths released from calcified cells can be seen around the non-calcified cells during the late period of the bloom (day 15).
F–H. Phase-contrast and epifluorescence micrograph images taken from fresh bloom samples: (F) A cluster of three non-calcified flagellated cells can be seen closely associated with an aggregate of coccoliths along with an isolated *E. huxleyi* calcified cell below (day 14 bag 3). (G) Chloroplast auto-fluorescence (490/630 nm, excitation/emission) for the cells in image (F). (H) Flagellated (arrow) non-calcified cell attached to coccolith debris. In a slightly lower plane, another non-calcified cell (slightly out of focus) can be seen next to the aggregate of coccoliths (magnification = 2500×).

and inner arm DHC1b), according to transcriptome analyses of 1N and 2N *E. huxleyi* cells performed by von Dassow and colleagues (2009).

Preliminary PCR tests using genomic DNA (gDNA) of different microalgae strains (Fig. 4, right panel) prior to analysing the mesocosm samples verified that all primer sets amplified both *E. huxleyi* control strains (Eh1 and Eh2), except the inner arm DHC1b primer set that only amplified Eh1. Non-specific amplification of *G. oceanica* (*Go*) and/or *Isochrysis* (*Ig*) was verified for the elongation factor 1α, histone H2A, phototropin homologue and inner arm DHC1b. Complementary tests performed at higher annealing temperatures (up to 62°C) did not improve the overall result (data not shown). Strict specificity to *E. huxleyi* was only obtained with Myb family transcription factor, false agglutinin homologue and putative DNA-6-adenine methyltransferase primer sets. No positive amplifications were obtained with the flagellated haptophyte *C. ericina* (*Co*). We also tested primer sets for two other genes (outer arm DHC-beta, putative cGMP protein kinase; see *Experimental procedures*) that successfully amplified in both *E. huxleyi* strains and *Go* (cGMP protein kinase only). However, we did not obtain positive amplification in the mesocosm samples, so these results were excluded from Fig. 4.

During the analysis of the M3 mesocosm samples (Fig. 4, left panel), we were able to amplify the elongation factor 1α in samples from all days, verifying both the presence of *E. huxleyi* throughout the bloom, as well as the quality of the sample extracts. cDNA products were notably smaller than genomic DNA products, due to the presence of introns (von Dassow *et al.*, 2009). Notably, we obtained two additional larger size amplicons on days 0, 11 and 14, one equalling the size of the DNA amplicon at ~ 500 bp and a larger one at ~ 800 bp. These bands persisted even after re-extracting new RNA from fresh duplicate samples. Among the primer sets strictly targeting *E. huxleyi* 1N-specific genes, we only observed successful amplification of mesocosm cDNA during early days (days 0 and 1) and during the peak bloom of 2N cells (days 11 and 14). All the other 1N primers followed the same general pattern, except for inner arm DHC1b and false agglutinin only amplifying on days 11 and 16 respectively. It was also noticeable that several 1N primer sets

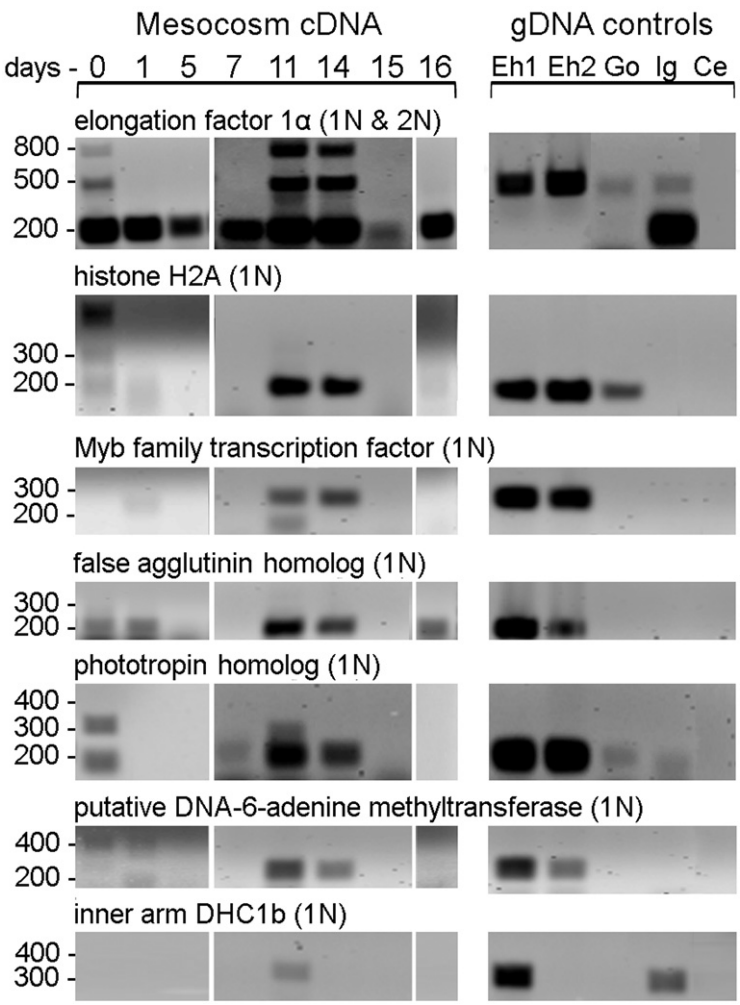


**Fig. 4.** RT-PCR detection of *E. huxleyi* transcripts (cDNA) in the nutrient replete M3 enclosure during days 0, 1, 5, 7, 11, 14, 15 and 16 (left panel). The elongation factor 1α gene is present in both 1N and 2N life cycle phases. All other genes (histone H2A, Myb family transcription factor, false agglutinin homologue, phototropin homologue, putative DNA-6-adenine methyltransferase and inner arm DHC1b) are haploid phase-specific according to von Dassow and colleagues (2009). Controls testing the specificity of the primers against genomic DNA (gDNA) from other prymnesiophytes (right panel): Eh1, *E. huxleyi* CCMP 374; Eh2, *E. huxleyi* CCMP1516; Go, *Gephyrocapsa oceanica* AC 396; Ig, *Isochrysis galbana* CCMP 1335; Ce, *Chrysochromulina ericina*. The positions of the molecular weight markers are shown on the left side of the gels.

amplified multiple bands in day 0, which was not circumvented in duplicate extractions.

## Discussion

### *COD-FISH probe specificity*

A critical aspect of our study was to assess *E. huxleyi* non-calcified cells in nature using the application of the COD-FISH method (Frada *et al*., 2006) using a new fluorescent probe (EG28-03) specifically targeting this species. Our probe (EG28-03) was designed against *E. huxleyi* and its close relative *G. oceanica* (Fig. S1), due to the fact that both cells can only be differentiated by a single nucleotide mutation in the 28S rRNA sequence (Liu *et al*., 2010; E.M. Bendif, I. Probert, J.R. Young, D.C. Schroeder and C. De Vargas, submitted) upon which no distinctive probe could be successfully developed. The lack of strict specificity of EG28-03 to *E. huxleyi* poses potential limitations while analysing field samples that contain both morphospecies. However, this caveat was not applicable to our study since *G. oceanica* cells are more associated with lower latitude water masses (Winter *et al*., 1994; Ziveri *et al*., 2004). In fact, we never detected calcified (2N) *Gephyrocapsa* cells, which are distinguishable from *E. huxleyi* due to the presence of a bridge spanning over the central area of coccoliths (Young *et al*., 2003; Frada *et al*., 2010). Thus, we are confident that our COD-FISH analyses specifically detected *E. huxleyi* cells in the mesocosm and surrounding fjord waters.

### *Bloom dynamics: abundance, distribution and ploidy nature of non-calcified cells*

Offshore mesocosms have been extensively used over the last couple of decades to reproduce *E. huxleyi* blooms and build a comprehensive understanding of factors promoting and controlling bloom succession. They have helped to define ecological and biogeochemical constraints, consequences, resilience to future atmospheric scenarios (e.g. Egge and Heimdal, 1994; Delille *et al*., 2005; Riebesell *et al*., 2008) and the interactions between

*E. huxleyi* and specific viruses (e.g. Bratbak *et al*., 1993; Jacquet *et al*., 2001; Martinez-Martinez *et al*., 2007; Pagarete *et al*., 2009). Here, we focused on a unique perspective by quantitatively surveying the presence and development of both calcified and non-calcified cells and detecting haploid cells (1N) during bloom successions. *Emiliania huxleyi* cells were quantified via the COD-FISH method (Frada *et al*., 2006) using a new *E. huxleyi*-specific probe, whereas haploid cells were detected via RT-PCR using haploid specific primers.

In order to provide ecological context on the background community, we first assessed the surrounding fjord water that was used to fill-up the mesocosm enclosures. Calcified 2N cells represented most of the *E. huxleyi* cells. However, non-calcifying *E. huxleyi* cells were also detected forming a minor ~ 10% fraction of the overall *E. huxleyi* community (Fig. 1). The ploidy nature of these cells is unclear. Nonetheless, the presence of 1N-specific transcripts detected during early mesocosm time points (Fig. 4, days 0 and 1) suggested that 1N cells may have been in fact present in fjord communities. Given that our focus was primarily on the analysis of the mesocosms, we did not survey the temporal dynamics and development of non-calcified cells. Nonetheless, complementary time series performed during a previous year in the same fjord area, as well as in the English Channel, also indicated that non-calcified cells (likely including 1N cells) follow parallel and relatively stable temporal dynamics with calcified 2N cell types, which always represented the most abundant phase (Fig. S2).

Daily N and P additions to the mesocosms promoted the formation of blooms of calcified 2N *E. huxleyi* cells (Fig. 2). In general, the magnitude of these blooms appeared to be dependent on P availability (Jacquet *et al*., 2001), while its final collapse, particularly in M3, was tightly regulated by *Eh*V infection, as demonstrated in companion studies performed during the same mesocosm survey (Pagarete *et al*., 2009; 2011; A. Vardi, L. Haramty, B. Van Mooy, H. Fredricks, S. Kimmance, A. Larsen and K. Bidle, pers. comm.). In these terms, P-limited enclosures (M2) yielded approximately half the cellular and viral densities compared with nutrient-replete enclosures (M3). Overall, non-calcified cells, including 1N cells, remained comparatively dilute. However, their relative abundance rose progressively during the stationary phase of calcified cells in M2 and at the end of exponential growth in M3 (Figs 2 and 3A–E), in parallel with *Eh*V burst.

Within this same period, we obtained prominent amplification signals for a diverse suite of 1N-specific gene markers from the community cDNA, thereby specifically diagnosing the presence of haploid cell types at specific time windows (days 0–1 and days 11–14; Fig. 4). In parallel water samples, we microscopically detected clusters of two or three small ($\leq 5\ \mu m$) autotrophic flagellates actively carrying remnants of *E. huxleyi* coccospheres (Fig. 3F–H, Video S1) and one of these flagellated cells detaching and swimming away from the coccoliths aggregate. These cells strongly resembled 1N *E. huxleyi* cells in terms of size, shape and swimming patterns (Green *et al*., 1996; Houdan *et al*., 2004; our laboratorial observations). Together with the aforementioned 1N molecular markers, we suggest that these flagellated cells represent recently produced 1N *E. huxleyi* cells that are still associated with the coccoliths of 'mother' 2N cells. As a consequence, our data support the induction of meiosis in *E. huxleyi* during peak bloom abundance and the beginning of viral demise. Indeed, the fact that our RT-PCR analysis was unable to detect haploid-specific transcripts during diploid cell bloom development (days 5 and 7), while sensitive enough to detect haploid-transcripts at pre-bloom non-calcified cell densities (days 0–1; 2–26 cells $ml^{-1}$), argues against haploid cells deriving solely from an initial inoculum. However, given the rarity of non-calcified cells relative to 2N calcified cells (Figs 1 and 2), we estimate that meiosis encompassed only a minor fraction of the 2N population (< 1%). To our knowledge, this is the first time that 1N *E. huxleyi* cells have been unequivocally 'unveiled' in nature.

An intriguing aspect of our survey was the rapid burst of non-calcified *E. huxleyi* during days 15 and 16 based on COD-FISH observations (Fig. 2). Given the decline of 1N-specific transcripts after day 15 (Fig. 4), where only a weaker false agglutinin homologue band was detected at day 16, and the concomitant increase in empty coccospheres without chlorophyll autofluorescence, we argue that the majority of these late-phase non-calcified cells were actually senescent 2N cells that had either lost or were in the act of losing their outer coccolith layers due to virally mediated cell death. Indeed, viral infection of *E. huxleyi* is known to elicit shedding of coccoliths and significantly reduces photosynthetic efficiency (Bidle *et al*., 2007; Frada *et al*., 2008). As such, our findings raise interesting questions as to the fate of the aforementioned 1N cells that had flourished within the 11–14 day time window. Perhaps they were more dilute among the cellular debris released during bloom collapse and therefore escaped detection or were preferentially lost through grazing. It is equally plausible that 1N cells underwent syngamy, preferentially mating and forming novel 2N genotypes. However, our level of analysis is insufficient to support either explanation and warrants further investigations into the ecological fate of haploid cells in late bloom phases.

### *Prevalence of non-calcified* E. huxleyi *cells within native populations*

Based on the fjord (Fig. 1 and Fig. S2), mesocosm (Fig. 2) and English Channel time series (Fig. S2) and

detection of non-calcified in ulterior field surveys (Campbell *et al*., 1994), it is clear that non-calcified *E. huxleyi* cells currently co-habit native populations. Thus, we now provide quantitative evidence that non-calcified cells, which likely contain 1N cells, generally contribute a minor fraction of the total *E. huxeyi* population with both life stages following parallel dynamics through time. This scenario contrasts with what has been reported for other coccolithophore species in which 2N and 1N cells (both producing distinct coccoliths and therefore readily identifiable), occupy different depth layers in the same geographic areas [*Helicosphaera carteri*, *Syracosphaera pulchra*, *C. mediterranea* (Cros, 2002)] or inter-change their relative dominance between seasons [*C. braarudii* (Okada and McIntyre, 1977; Balestra *et al*., 2004)]. Given *E. huxleyi* is the most dominant and widespread coccolithophore morphospecies (McIntyre and Bé, 1967; Campbell *et al*., 1994), this distinction between the dynamics of 2N and 1N cells of *E. huxleyi* and other coccolithophores may indicate a selective advantage to maintain both life cycle phases in the same water mass. Indeed, a recurrent hypothesis for the maintenance of a haplodiplontic life cycle is the idea that each phase occupies distinct niches, providing opportunities for species to exploit different resources (Valero *et al*., 1992; Mable and Otto, 1998). Niche separation in most coccolithophores appears to reflect physical separation on spatial and temporal scales, as mentioned above. However, as demonstrated in our study, haploid and diploid phases can overlap in time or space, perhaps complementing the respective ecological potential with minimal intra-specific competition due to distinct physiological attributes. In this case, beneficial properties of 1N *E. huxleyi* cells, like swimming abilities, mixotrophy (Rokitta *et al*., 2011) and viral resistance (Frada *et al*., 2008), could account for the maintenance of a stable coexistence between both life cycle phases, while ultimately contributing to the overall success of *E. huxleyi* in modern oceans.

### *Life cycle turnover: evidence and implications*

A particularly noteworthy finding in our study was the apparent induction of meiosis during the end of exponential and stationary phases of bloom development, as supported by the timing of morphological and molecular markers. Which conditions or cues promoted this process? Current knowledge of factors promoting coccolithophore (or even Haptophyte) life cycle phase transitions, including meiosis and syngamy, is extremely vague (see Houdan *et al*., 2004 and Noël *et al*., 2004, for reviews). A few reports suggest that in the *Pleurochrysidaceae*, a family of coastal coccolithophores, temperature, light and nutrient availability critically promote phase changes (Leadbeater, 1971; Gayral and Fresnel, 1983). Both nutrient availability and quality also appear to be fundamental for sex and meiosis in *Calyptrosphaera sphaeroidea* (Noël *et al*., 2004). In contrast, the key trigger of syngamy in the oceanic species *C. braarudii* may be turbulence (Houdan *et al*., 2004; 2006). Current information on *E. huxleyi* is equally meagre. Klaveness's (1972) original descriptions state that flagellated, 1N cells are produced by senescent calcified 2N cells, implicating that nutrient starvation promotes meiosis. More recently, Laguna and colleagues (2001) suggested that meiosis was induced by changes in medium viscosity (i.e. agar-plating). However, these authors did not provide reliable cytological evidence for newly formed 1N cells, which instead closely resembled bacterial contaminants. These results should therefore be considered with caution. More recently, Frada and colleagues (2008) observed that 1N cells were produced after *Eh*V-mediated collapse of 2N cultures, suggesting that meiosis could be triggered in response to viral infection. This mechanism, coined the 'Cheshire Cat' escape strategy, argues that host cells switch to the 1N and *Eh*V resistant stage via meiosis, enabling species survival and long-term persistence. Our observations during the Bergen 2008 mesocosm experiments are consistent with this model, namely that the development of 1N cells coincided with massive *Eh*V proliferation and the death of diploid host cells. Whether meiosis was directly or indirectly triggered in response to viruses is uncertain. However, it seems plausible that meiosis could be induced by chemical cues released during infection, possibly by infected cells during or upon cell lysis, and sensitizing healthy cells to produce *Eh*V-resistant haploids in order to escape viral pressure and arguably constrain viral proliferation (Frada *et al*., 2008; Bidle and Vardi, 2011). Candidate molecules with such potential may include reactive oxygen species (ROS) and bioactive sphingolipids (and/or derived products), since they are both produced and dispersed during *Eh*V infection (Evans *et al*., 2006; Vardi *et al*., 2009; A. Vardi, L. Haramty, B. Van Mooy, H. Fredricks, S. Kimmance, A. Larsen and K. Bidle, pers. comm.) and they are known elicitors of sexual life cycle transition in other organisms, including dinoflagellates (Vardi *et al*., 1999), colonial green algae (Nedelcu *et al*., 2004; Nedelcu, 2005), slime moulds (Ameisen, 2002) and yeast (Cowart *et al*., 2006). The effectiveness of these molecules on inducing *E. huxleyi* life cycling warrants further investigation. Of course, it is also possible that induction of meiosis was caused by factors such us starvation exerted during blooms peak or even by the exposure to meiosis-promoting factors that could accumulate at high cell densities and elicit life cycle transition like in yeast (Hayashi *et al*., 1998). Alternatively, meiosis could be regulated by an internal biological clock. In fact, it has been repeatedly observed the

seemingly spontaneous production of 1N *E. huxleyi* cells within healthy 2N *E. huxleyi* cultures within three and nine months after isolation (Houdan *et al*., 2004). As in many other living organisms (Costas and Varela, 1989; Lüning and Kadel, 1993; Montresor and Lewis, 2006), endogenous cellular rhythms controlling growth and reproduction could apply to *E. huxleyi*.

### *Final remarks*

Detailed knowledge of *E. huxleyi* life cycle transitions is fundamental for a holistic comprehension of its ecological and biogeochemical significance, resilience and evolution. Using morphological and molecular gene markers we provided novel insights into the life phase dynamics and life cycle transitions of natural *E. huxleyi* populations and during bloom succession. There are many open questions that remain, such as the maintenance of a stable coexistence between life cycle phases during inter-bloom periods, the trigger(s) of meiosis, the fate of haploid cells released into the environment, as well as the timing and mode of syngamy and its impact on *E. huxleyi* and EhV evolution. Comprehensive approaches spanning from culturing to field surveys, where detailed microscopy (COD-FISH), gene expression and meiosis- or mating-specific molecules can be assessed and tested, provide an immense platform to fully unveil the life cycle intricacies of this ecologically and biogeochemically important phytoplankton species.

## Experimental procedures

### *Experimental set-up*

Mesocosms designed to monitor *E. huxleyi* blooms were carried out for 17 days (5–21 June 2008) in the Raunefjorden, western Norway [60°22.1′N; 5°28.1′E; as previously described in Pagarete *et al*. (2011)]. Briefly, 11 $m^3$ transparent enclosures were mounted on floating frames and filled with unfiltered seawater from the surrounding fjord. Enclosures were enriched daily with $NaNO_3$ and $K_2HPO_4$ at either 15N:1P (1.5 μM $NaNO_3$: 0.1 μM $K_2HPO_4$; M3-replete) or 75N:1P ratios (1.5 μM $NaNO_3$: 0.02 μM $K_2HPO_4$; M2-P-limited). Surface water samples from each enclosure were collected at 06:00 h. Prior to the mesocosm experiment, samples were also collected from the fjord (0, 5 and 10 m) using a Niskin bottle in order to provide context on the background community. Samples were brought to the laboratory adjacent to the mesocosms and processed for subsequent COD-FISH and gene expression analyses (see below). Fresh samples were also monitored daily with a microscope (Leica DMR type 020–525.024 straight microscope) for microalgae diversity. Photographic images were taken with a standard digital camera (SONY cyber-shot 5.1 mega pixels) directly through the microscope eyepiece. *Emiliania huxleyi* virus (*Eh*Vs) counts used in our study are derived from those published in Pagarete and colleagues (2011).

### *COD-FISH probe design, testing and analysis*

*Emiliania huxleyi* interchanges between calcified and non-calcified forms during its life cycle (e.g. Green *et al*., 1996). Calcified cells are clearly visible and readily identifiable by cross-polarizing microscopy (Frada *et al*., 2006; 2010). Non-calcified cells, however, are undistinguishable from other small microalgae using optical methods. For this reason, we designed a new fluorescence *in situ* hybridization (FISH) oligonucleotidic probe to specifically target and highlight non-calcified *E. huxleyi* cells within natural phytoplankton assemblages. This novel probe (EG28-03, 5′-TAAAGCCCCGCTCCCGGGTT-3′) was designed against the large ribosomal subunit (28S) of both *E. huxleyi* and the close relative and nearly undistinguishable at the ribosomal level, *Gephyrocapsa oceanica* (Liu *et al*., 2010; E.M. Bendif, I. Probert, J.R. Young, D.C. Schroeder and C. De Vargas, submitted) with the ARB software (Ludwig *et al*., 2004). The probe was labelled with horseradish peroxidase (HRP) for enhanced fluorescence labelling (Not *et al*., 2002). We then used the COD-FISH method that couples FISH with cross-polarizing microscopy, thereby allowing the specific and simultaneous quantitative assessment of calcified and non-calcified *E. huxleyi* cells in field samples (Frada *et al*., 2006).

Prior applying the probe in field samples, we tested its specificity against a wide array of cultured microalgae (Fig. S1) and fine-tuned hybridization conditions. Briefly, 5–10 ml of each culture and 5–200 ml of mesocosm samples (higher volumes were processed with low cell density samples, whereas smaller volumes were used for high density samples) were fixed in triplicate with 1% paraformaldehyde 6 mM $Na_2CO_3$ for 1 h at 4°C, then vacuum filtered onto 25 mm anodisc filters (Whatman, Maidstone, Kent, UK), dehydrated in a ethanol series (50%, 80% and 100%) and covered with 1 ml of pre-warmed 1% liquid gelatine according to the original protocol (Frada *et al*., 2006). After drying the filters were stored at −80°C. EG28-03 probe hybridization was performed with representative sections of the filters at 40°C for 12 h in 45% formamide hybridization buffer. Washing steps were performed at 42°C with NaCl adjusted to 50 mM. Labelled cells were simultaneously enumerated by epifluorescence microscopy (495/520 nm excitation/emission for FITC fluorescence) and cross-polarized microscopy using an Olympus BX51 microscope equipped with a mercury lamp and basic Nomarski setup (Olympus, Japan). Pictures were taken with a RT-Slider Spot cooled charge coupled device digital camera (Diagnostic Instruments, Sterling Heights, MI, USA).

### *RNA isolation, cDNA generation and PCR conditions*

Sample volumes harvested from M3 enclosure for RNA analysis varied depending on collection day: 0.5 l, day 0; 1 l, days 1 and 5; 2 l, day 7; 1.5 l, days 11, 14, 15 and 16. Cells were filtered under gentle vacuum onto 47 mm diameter, 0.8 μm pore-size white AAWP mixed cellulose ester filters (Millipore, Billerica, MA, USA) after prescreening with 100 μm pore-size Nitex mesh to remove large zooplankton. Collected biomass was scraped off the filters with a clean razor blade into a sterile Petri dish, resuspended in 0.2 μm-filtered sea-

water and transferred to a sterile microfuge tube. Cells were pelleted via centrifugation (2 min, max. speed, room temperature), frozen immediately in liquid $N_2$ and stored at −80°C until processing.

For RNA extraction, 1 ml of TRI reagent (Applied Biosystems/Ambion, Austin, TX, USA) was added to sample pellets and incubated for 5 min at room temperature, followed by the addition of 100 μl of 1-bromo-3-chloropropane (BCP, Molecular Research) and incubation for 10 min. Samples were centrifuged (12 000 *g* at 4°C for 15 min), the aqueous phase was transferred to new tubes, and mixed with 0.5 volume of 100% ethanol. Extracts were applied to RNeasy columns (RNAeasy Plant Minikit, Qiagen, Valencia, CA, USA) and processed according to the manufacturer's recommendations. RNA was eluted in 40 μl of RNase-free water. RNA quantity and quality was assessed with a Nanodrop spectrophotometer (Thermo Fisher Scientific, Walthem, MA, USA), with 260:280 ratios consistently ≈ 2. Approximately 4 μg of RNA for each sample was rendered free from possible contaminating DNA with one round of Turbo DNase treatment (Applied Biosystems/Ambion) following manufacturer's recommendations. The treated RNA was again quantified using a Nanodrop and the presence of contaminating DNA was assessed via PCR using Invitrogen DNA Taq polymerase (Invitrogen, Carlsbad, CA, USA) and an 18S general primer (Medlin *et al*., 1988). All RNA samples (~ 1μg) were reverse transcribed into cDNA using the SuperScript III first-strand synthesis system (Invitrogen, Carlsbad, CA, USA) for 50 min at 55°C using oligo-dT primers following the manufacturer's protocol. First strand cDNA was used for qualitative PCR detection of selected and constitutively expressed *E. huxleyi* genes (von Dassow *et al*., 2009, Table S1). We specifically targeted one gene expressed in both 1N and 2N phase, the elongation factor 1α (cluster ID, GS00217); all the other markers specifically targeted 1N cells: histone H2A (cluster ID, GS10455), Myb family transcription factor (cluster ID, GS00273), false agglutinin homologue (cluster ID, GS05223), phototropin homologue (cluster ID, GS00920), putative DNA-6-adenine methyltransferase (cluster ID, GS02990), flagellar dynein inner arm heavy chain DHC1b (cluster ID, GS02579), flagellar dynein outer arm heavy chain DHCb (cluster ID, GS00667) and a possible cGMP protein kinase (cluster ID, GS00910). PCR amplifications were performed using recombinant Taq Polymerase (Invitrogen, Carlsbad, CA, USA) with 1 mM $MgCl_2$, 0.2 mM dNTPs, 0.2 μM of each primer (see von Dassow *et al*., 2009) and 5% of dimethylsulfoxide (Sigma-Aldrich, St. Louis, MO, USA). The thermocycler protocol was as follows: initial denaturation at 95°C for 5 min; 40 cycles of 45 s denaturation at 95°C, 45 s of annealing at 60°C (except for actin which used a 55°C annealing temperature), and 90 s extension at 72°C; 10 min extension at 72°C. 1% agarose gel electrophoresis was used to assess amplifications.

Prior applying the primer sets on the mesocosm samples we tested their specificity against DNA extracts of several microalgae strains. Tests were performed against cell lysates from two *E. huxleyi* strains (CCMP374 and CCMP1516), two phylogenetic relatives, *Gephyrocapsa oceanica* (AC396) and *Isochrysis galbana* (CCMP1335), and a flagellated haptophyte, *Chrysochromulina ericina* (Parke and Manton, University of Bergen Culture Collection). PCR amplifications were performed under the same conditions described above.

## Acknowledgements

We acknowledge mesocosm organizers, W. Wilson, M. Allen, S. Kimmance and A. Aadnesen, and participants for help, discussions and advice. We acknowledge D. Hinz for collecting samples from the Raunefjord in 2007 and the Roscoff culture collection staff for providing cultures for COD-FISH testing. Lastly, we acknowledge three anonymous reviewers who provided valuable feedback and guidance that strengthened the final version of the manuscript. Support to M.J.F. was provided by a PhD fellowship from the '*Fundação Para a Ciência e para a Tecnologia*' (Portugal), an Algal node student scholarship ('Marine Genomics Europe' – European Commission contract No. GOCE-CT-2004-505403) and the Cd-ToxCoN project (FCT: PTDC/MAR/102800/2008). Overall support to M.J.F., I.P. and C.d.V. was provided by the EU Funding Agencies from the ERA-net program Biodiversa, under the *BioMarKs* project, and by the EU 7th Framework Program *EPOCA* (European Project on Ocean Acidification) under grant agreement 211384. Support to K.D.B. was provided by grants from the US National Science Foundation (IOS-0717494; OCE-1061883).

## References

Ameisen, J.C. (2002) On the origin, evolution, and nature of programmed cell death: a timeline of four billion years. *Cell Death Differ* **9:** 367–393.

Balestra, B., Ziveri, P., Monechi, S., and Troelstra, S. (2004) Coccolithophorids from the southeast Greenland margin (northern north atlantic): production ecology and the surface sediment record. *J Nannoplankton Res* **50:** 23–34.

Bidle, K.D., and Vardi, A. (2011) chemical arms race at sea mediates algal host–virus interactions. *Curr Opin Microbiol* **14:** 1–9.

Bidle, K.D., Haramaty, L., Ramos, J.B.E., and Falkowski, P. (2007) Viral activation and recruitment of metacaspases in the unicellular coccolithophore, *Emiliania huxleyi*. *Proc Natl Acad Sci USA* **104:** 6049–6054.

Billard, C. (1994) Life cycles. In *The Haptophyta Algae*. Green, J.C., and Leadbeater, B.S.C. (eds). Oxford, UK: Clarendon Press, pp. 167–186.

Bratbak, G., Egge, J., and Heldal, M. (1993) Viral mortality of the marine alga *Emiliania huxelyi* (Haptophyceae) and the termination of the algal bloom. *Mar Ecol Prog Ser* **93:** 39–48.

Brown, C.W., and Yoder, J.A. (1994) Coccolithophorid blooms in the global ocean. *J Geophys Res* **99:** 7467–7482.

Campbell, L., Shapiro, L.P., and Haugen, E. (1994) Immunochemical characterization of eukaryotic ultraplankton from the Atlantic and Pacific Oceans. *J Plankton Res* **16:** 35–51.

Charlson, R.J., Lovelock, J.E., Andreae, M.C., and Warren, S.G. (1987) Oceanic phytoplankton, atmospheric sulfur, cloud albedo and climate. *Nature* **326:** 655–661.

Costas, E., and Varela, M. (1989) Circannual rhythm in cyst formation and growth rates in the dinoflagellate *Scrippsiella trochoidea* Stein. *Chronobiologica* **16:** 265–270.

Cowart, L.A., Okamoto, Y., Lu, X., and Hannun, Y.A. (2006) Distinct roles for *de novo* versus hydrolytic pathways of sphingolipid biosynthesis in *Saccharomyces cerevisiae*. *Biochem J* **393:** 733–740.

Cros, L. (2002) *Planktonic Coccolithophores of the NW Mediterranean*. Barcelona, Spain: Universitat de Barcelona.

von Dassow, P., Ogata, H., Probert, I., Wincker, P., Da Silva, C., Audic, S., *et al*. (2009) Transcriptome analysis of functional differentiation between haploid and diploid cells of *Emiliania huxleyi*, a globally significant photosynthetic calcifying cell. *Genome Biol* **10:** R114.

Delille, B., Harlay, J., Zondervan, I., Jacquet, S., Chou, L., Wollast, R., *et al*. (2005) Response of primary production and calcification to changes of $pCO_2$ during experimental blooms of the coccolithophorid *Emiliania huxleyi*. *Global Biogeochem Cycles* **19:** GB2023.

Egge, J.K., and Heimdal, B.R. (1994) Blooms of phytoplankton including *Emiliania huxleyi* (*Haptophyta*). Effects of nutrient supply in different N : P ratios. *Sarsia* **79:** 333–348.

Evans, C., Malin, G., Mills, G.P., and Wilson, W.H. (2006) Viral infection of *Emiliania huxleyi* (*Prymnesiophyceae*) leads to elevated production of reactive oxygen species. *J Phycol* **42:** 1040–1047.

Frada, M., Not, F., Probert, I., and de Vargas, C. (2006) $CaCO_3$ optical detection with fluorescent *in situ* hybridization: a new method to identify and quantify calcifying microorganisms from the oceans. *J Phycol* **42:** 1162–1169.

Frada, M., Probert, I., Allen, A.E., Wilson, W.H., and de Vargas, C. (2008) The 'Cheshire Cat' escape strategy of the coccolithophore *Emiliania huxleyi* in response to viral infection. *Proc Natl Acad Sci USA* **105:** 15944–15949.

Frada, M., Young, J., Cachão, M., Lino, S., Martins, A., Narciso, A., *et al*. (2010) A guide to extant coccolithophores (*Calcihaptophycidae, Haptophyta*) using light microscopy. *J Nannoplankton Res* **31:** 58–112.

Gayral, P., and Fresnel, J. (1983) Description, sexualité et cycle de développement d'une nouvelle Coccolithophoracée (*Prymnesiophyceae*): *Pleurochrysis pseudoroscoffensis* sp. nov. *Protistologica* **19:** 245–261.

Green, J.C., Course, P.A., and Tarran, G.A. (1996) The life-cycle of *Emiliania huxleyi*: a brief review and a study of relative ploidy levels analysed by flow cytometry. *J Mar Syst* **9:** 33–44.

Hagino, K., Bendif, E.M., Young, J., Kogame, K., Takano, Y., Probert, I., *et al*. (2011) New evidence for morphological and genetic variation in the cosmopolitan coccolithophore *Emiliana huxleyi* (*Prymnesiophyceae*) from the cox1b-ATP4 genes. *J Phycol* **47:** 1164–1176.

Hayashi, M., Ohkuni, K., and Yamashita, I. (1998) An extracellular meiosis-promoting factor in *Saccharomyces cerevisiae*. *Yeast* **14:** 617–622.

Holligan, P.M., Violler, M., Harbour, D.S., Camus, P., and Champagne-Philippe, M. (1983) Satellite and ship studies of coccolithophore production along a continental shelf edge. *Nature* **304:** 339–342.

Houdan, A., Billard, C., Marie, D., Not, F., Saez, A., Young, G., and Probert, I. (2004) Holococcolithophores-heterococcolithophores (*Haptophyta*) life cycles: flow cytometry analysis of relative ploidy levels. *System Biodivers* **1:** 453–465.

Houdan, A., Probert, I., Van Lenning, K., and Lefebvre, C. (2005) Comparison of photosynthetic responses in diploid and haploid life-cycle phases of *Emiliania huxleyi* (*Prymnesiophyceae*). *Mar Ecol Prog Ser* **292:** 139–146.

Houdan, A., Probert, I., Zatylny, C., Véron, B., and Billard, C. (2006) Ecology of oceanic coccolithophores. I. nutritional preferences of the two stages in the life cycle of *Coccolithus braarudii* and *Calcidiscus leptoporus*. *Aquat Microb Ecol* **44:** 291–301.

Iglesias-Rodriguez, M.D., Schofield, O.M., Batley, J., Medlin, L.K., and Hayes, P.K. (2006) Intraspecific genetic diversity in the marine coccolithophore *Emiliania huxleyi* (*Prymnesiophyceae*): the use of microsatellite analysis in marine phytoplankton population studies. *J Phycol* **42:** 526–536.

Jacquet, S., Heldal, M., Iglesias-Rodriguez, D., Larsen, A., Wilson, W., and Bratbak, G. (2001) Flow cytometric analysis of an *Emiliana huxleyi* bloom terminated by viral infection. *Aquat Microb Ecol* **27:** 111–124.

Klaveness, D. (1972) *Coccolithus huxleyi* (Lohm.) Kamptn. II. The flagellate cell. aberrant cell types, vegetative propagation and life cycles. *Br Phycol J* **7:** 309–318.

Laguna, R., Romo, J., Read, B.A., and Wahlund, T.M. (2001) Induction of phase variation events in the life cycle of the marine coccolithophorid *Emiliania huxleyi*. *Appl Environ Microbiol* **67:** 3824–3831.

Leadbeater, B.S.C. (1971) Observations on the life history of the haptophyceaen alga *Pleurochrysis scherffellii* with special reference to the microanatomy of the different types of motile cells. *Ann Bot* **35:** 429–439.

Liu, H., Aris-Brosou, S., Probert, I., and de Vargas, C. (2010) A timeline of the environmental genetics of the haptophytes. *Mol Biol Evol* **27:** 171–176.

Lohmann, H. (1902) Die Coccolithophoridae, eine Monographie der Coccolithen bildenden flagellaten, zugleich ein beitrag zur kenntnis des mittelmeerauftriebs. *Archiv für Protistenkunde* **1:** 89–165.

Ludwig, W., Strunk, O., Westram, R., Richter, L., Meier, H., *et al*. (2004) ARB: a software environment for sequence data. *Nucleic Acids Res* **32:** 1363–1371.

Lüning, K., and Kadel, P. (1993) Daylength range for circannual rhythmicity in *Pterygophora californica* (*Alariaceae, Phaeophyta*) and synchronization of seasonal growth by daylength cycles in several other brown algae. *Phycologia* **32:** 379–387.

Mable, B.K., and Otto, S.P. (1998) The evolution of life cycles with haploid and diploid phases. *Bioessays* **20:** 453–462.

McIntyre, A., and Bé, A.W. (1967) Modern coccolithophoridae of the Atlantic Ocean. I. Placoliths and cyrtoliths. *Deep Sea Res* **4:** 561–597.

Malin, G., and Steinke, M. (2004) Dimethyl sulfide production: what is the contribution of the coccolithophores? *Coccolithophores: From the Molecular Processes to Global Impact*. Thierstein, H.R., and Young, J.R. (eds). New York, USA: Springer Verlag, pp. 127–164.

Martinez-Martinez, J., Schroeder, D., Larsen, A., Bratbak, G., and Wilson, W. (2007) Molecular dynamics of *Emiliania huxleyi* and cooccurring viruses during two separate mesocosm studies. *Appl Environ Microbiol* **73:** 554–562.

Medlin, L.K., Elwood, H.J., Stickel, S., and Sogin, M.L. (1988) The enzymatic characterization of enzymatically amplified eukaryotic 16S-like rRNA-coding regions. *Gene* **71:** 491–499.

Montresor, M., and Lewis, J. (2006) Phases, stages, and shifts in the life cycles of marine phytoplankton. In *Algal Cultures, Analogues of Blooms and Applications*. Subba Rao, D. (ed.). Enfield, USA: Science Publishers, pp. 91–129.

Nedelcu, A.M. (2005) Sex as a response to oxidative stress: stress genes co-opted for sex. *Proc R Soc Lond B Biol Sci* **272:** 1935–1940.

Nedelcu, A.M., Marcu, O., and Michod, R.E. (2004) Sex as a response to oxidative stress: a twofold increase in cellular reactive oxygen species activates sex genes. *Proc R Soc Lond B Biol Sci* **271:** 1591–1596.

Noël, M.-H., Kawachi, M., and Inouye, I. (2004) Induced dimorphic life cycle of a coccolithophorid, *Calyptrosphaera sphaeroidea* (*Prymnesiophyceae, Haptophyta*). *J Phycol* **40:** 112–129.

Not, F., Simon, N., Biegala, I., and Vaulot, D. (2002) Application of fluorescent in situ hybridization coupled with tyramide signal amplification (FISH-TSA) to assess eukaryotic picoplankton composition. *Aquat Microb Ecol* **28:** 157–166.

Okada, H., and McIntyre, A. (1977) Modern coccolithophores of the Pacific and North Atlantic Oceans. *Micropaleontology* **23:** 1–55.

Paasche, E. (2001) A review of the coccolithophorid *Emiliania huxleyi* (*Prymnesiophyceae*), with particular reference to growth, coccolith formation, and calcification photosynthesis interactions. *Phycologia* **40:** 503–529.

Pagarete, A., Allen, M.J., Wilson, W.H., Kimmance, S.A., and de Vargas, C. (2009) Host–virus shift of the sphingolipid pathway along an *Emiliania huxleyi* bloom: survival of the fattest. *Environ Microbiol* **11:** 2840–2848.

Pagarete, A., Le Corguillé, G., Tiwari, B., Ogata, H., de Vargas, C., Wilson, W.H., and Allen, A.E. (2011) Unveiling the transcriptional features associated with coccolithvirus infection of natural *Emiliania huxleyi* blooms. *FEMS Microbiol Ecol* **78:** 555–564.

Rhodes, L.L., Peake, B.M., MacKenzie, A.L., and Marwick, S. (1995) Coccolithophores *Gephyrocapsa oceanica* and *Emiliania huxleyi* (*Prymnesiophyceae* = *Haptophyceae*) in New Zealand's coastal waters: Characteristics of blooms and growth in laboratory culture. *NZ J Mar Freshwater Res* **29:** 345–357.

Riebesell, U., Bellerby, R.G.J., Grossart, H.P., and Thingstad, F. (2008) Mesocosm $CO_2$ perturbation studies: from organism to community level. *Biogeosciences* **5:** 1157–1164.

Rokitta, S.D., de Nooijer, L.J., Trimborn, S., de Vargas, C., Rost, B., and John, U. (2011) Transcriptome analyses reveal differential gene expression patterns between the life-cycle stages of *Emiliania huxleyi* (*Haptophyta*) and reflect specialization to different ecological niches. *J Phycol* **47:** 829–838.

Rost, B., and Riebesell, U. (2004) Coccolithophores calcification and the biological pump: reponse to environmental changes. In *Coccolithophores: From the Molecular Processes to Global Impact*. Thierstein, H.R., and Young, J.R. (eds). New York, USA: Springer Verlag, pp. 99–125.

Shapiro, L.P., Campbell, L., and Haugen, E.M. (1989) Immunochemical recognition of phytoplankton species. *Mar Ecol Prog Ser* **57:** 219–224.

Tyrrell, T., and Merico, A. (2004) *Emiliania huxleyi*: bloom observation and the conditions that induce them. In *Coccolithophores: From the Molecular Processes to Global Impact*. Thierstein, H.R., and Young, J.R. (eds). New York, USA: Springer Verlag, pp. 75–97.

Valero, M., Richerd, S., and Perrot, V. (1992) Evolution of alternation of haploid and diploid phases in life cycles. *Trends Ecol Evol* **7:** 25–29.

Vardi, A., Berman-Frank, I., Rozenberg, T., Hadas, O., Kaplan, A., and Levine, A. (1999) Programmed cell death of the dinoflagellate *Peridinium gatunense* is mediated by $CO_2$ limitation and oxidative stress. *Curr Biol* **9:** 1061–1064.

Vardi, A., Van Mooy, B.A.S., Fredricks, H.F., Popendorf, K.J., Ossolinski, J.E., Haramaty, L., and Bidle, K.D. (2009) Viral glycosphingolipids induce lytic infection and cell death in marine phytoplankton. *Science* **329:** 861–865.

Westbroek, P., Brown, C.W., Van Bleijswijk, J., Brownlee, C., Brummer, G.J., Cote, M., *et al*. (1993) A model system approach to biological climate forcing: the example of *Emiliania huxleyi*. *Glob Planet Change* **8:** 27–46.

Winter, A., Jordan, R.W., and Roth, P.H. (1994) *Biogeography of Living Coccolithophores in Ocean Waters*. Cambridge, UK: Cambridge University Press.

Young, J., Geisen, M., Cros, L., Kleijne, A., Sprengel, C., Probert, I., and Østergaard, J. (2003) A guide to extant coccolithophore taxonomy. *J Nannoplankton Res Spec Issue* **1:** 125 pp.

Ziveri, P., Baumann, K.-H., Böckel, B., Bollmann, J., and Young, J.R. (2004) Biogeography of selected holocene coccoliths in the Atlantic Ocean. In *Coccolithophores – From Molecular Processes to Global Impact*. Thierstein, H.R., and Young, J.R. (eds). Berlin, Germany: Springer, pp. 403–428.

## Supporting information

Additional Supporting Information may be found in the online version of this article:

**Fig. S1.** Specificity test of the probe EG28-03. All the tested strains are visualized by epifluorescence hybridized both with the EG28-03 probe and a general haptophyta probe (Pym-02, Simon *et al*. 2000) and by cross-polarization. Haptophytes: A. *Emiliania huxleyi* RCC1216 (mixture of diploid and haploid cells); B. *E huxleyi* RCC1249 (mixture of diploid and haploid cells); C. *Gephyrocapsa oceanica* RCC1315 (mixture of diploid and haploid cells); D. *Isochrysis galbana* RCC1347; E. *I. galbana* RCC1349; F. *Pleurochrysis carterae* RCC1402; G. *Algirosphaera robusta* RCC1128; H. *Syracosphaera pulchra* RCC1131; I. *Prymnesium* sp. RCC1348; J. *Chrysochromulina* sp. RCC1186; K. *Phaeocystis* sp. CCMP2496; L. *Pavlova* sp. RCC1543. Non-haptophytes (only tested with EG28-03): M. *Rhodomonas salina* RCC20; N. *Skeletonema costatum* RCC70; O. *Amphidinium carterae* RCC88; P. *Dunaliella tertiolecta* RCC6. Scale bar = 5 μm.

**Fig. S2.** E. huxleyi calcified and non-calcified cell dynamics in the English Chanel (Astan station, offshore Roscoff, France) and Raunefjord (Bergen, Norway).
**Table S1.** List of haploid-diploid and haploid specific gene primers.
**Video S1.** Movie of two autotrophic flagellated swimming bound to a common coccolith agglomerate during day 14 in mesocosm 3. Cells were visualized by phase contrast. The movie was taken with a standard digital camera (SONY cyber-shot 5.1 mega pixels) directly through the microscope eyepiece. Magnification = 2500×.

Please note: Wiley-Blackwell are not responsible for the content or functionality of any supporting materials supplied by the authors. Any queries (other than missing material) should be directed to the corresponding author for the article.